Mechanism of Hydrogen Peroxide Dismutation by a Dimanganese Catalase Mimic: Dominant Role of an Intramolecular Base on Substrate Binding Affinity and Rate Acceleration

A. E. M. Boelrijk and G. C. Dismukes*

Department of Chemistry, Henry H. Hoyt Laboratory, Princeton University, Princeton, New Jersey, 08540

Received October 5, 1999

Several modifications of the manganese coordination environment and oxidation states of a family of synthetic dimanganese complexes have been introduced in search of the structural features that promote high rates of hydrogen peroxide dismutation (catalase activity). The X-ray structure of reduced catalase (*T. thermophilus*) reveals a dimanganese(II,II) site linked by three bridges: μ_{13}-glutamate$^-$, μ-OH$^-$, and μ-OH$_2$. The roles of a bridging hydroxide vs μ-aqua and the carboxylate have been examined in the reduced Mn_2(II,II) complexes, $[(L^{1,2})Mn_2(\mu\text{-}O_2CCH_3)(\mu\text{-}X)]^{2+}$ for X$^-$ = OH$^-$ (**7A**) or X = H$_2$O (**1**−**4**), and their oxidized Mn_2(III,III) analogues, $[(L^{1,2})Mn_2(\mu\text{-}O)(O_2CCH_3)(OH)]^+$ (**6**) (L^1 is *N*,*N*,*N*′,*N*′-tetrakis(2-methylenebenzamidazolyl)-1,3-diaminopropan-2-ol, and L^2 is the tetrakis-N-ethylated analogue of L^1, which has all amine protons replaced by ethyl groups). The steady-state catalase rate is first-order in concentration of both substrate and reduced catalyst and saturates at high peroxide concentrations in all cases, confirming peroxide/catalyst complex formation. No catalyst decomposition is seen after >2000 turnovers. Catalysis proceeds via a ping−pong mechanism between the Mn_2(II,II/III,III) redox states, involving complexes **6** and **7A**/**7A**′. The Mn_2(III,IV) oxidation state was not active in catalase activity. Replacement of the μ-aqua bridge by μ-hydroxide eliminates a kinetic lag phase in production of the O_2 product, increases the affinity for substrate peroxide in the rate-limiting step as seen by a 5-fold decrease in the Michaelis constant (K_M), and accelerates the maximum rate (k_{cat}) by 6.5-fold. The kinetic and spectroscopic data are consistent with substrate deprotonation by the hydroxide bridge, yielding a hydroperoxyl bridge coordinated between the Mn ions (μ,η_2 geometry, "end-on") as the basis for catalysis: μ-OH$^-$ + H_2O_2 → μ-O_2H^- + H_2O. Binding of a second hydroxide ion to **7A** causes a further increase in k_{cat} by 4-fold with no further change in substrate affinity (K_M). By contrast, free (noncoordinating) bases in solution have no effect on catalysis, thus establishing intramolecular sites for both functional hydroxide anions. Solution structural studies indicate that the presence of 2−5 equiv of hydroxide in solution leads to formation of a bishydroxide species, $[(L^{1,2})Mn_2(\mu_{13}\text{-}O_2CCH_3)(OH)_2]$, which in the presence of air or oxygen auto-oxidizes to yield complex **6**, a Mn_2(III,III)(μ-O) species. Complex **6** oxidizes H_2O_2 to O_2 without a kinetic lag phase and is implicated as the active form of the oxidized catalyst. A maximum increase by 240-fold in catalytic efficiency (k_{cat}/K_M = 700 s^{-1} M^{-1}) is observed with the bishydroxide species versus the aquo complex **1**, or only 800-fold less efficient than the enzyme. Deprotonation of the amine groups of the chelate ligand L was shown not to be involved in the hydroxide effects because identical results were obtained using the catalyst with tetrakis(*N*-ethylated)−L. Uncoupling of the Mn(II) spins by protonation of the alkoxyl bridge (LH) was observed to lower the catalase activity. Comparisons to other dimanganese complexes reveals that the Mn_2(II,II)/Mn_2(III,III) redox potential is not the determining factor in the catalase rate of these complexes. Rather, rate acceleration correlates with the availability of an intramolecular hydroxide for substrate deprotonation and with binding of the substrate at the bridging site between Mn ions in the reductive O−O bond cleavage step that forms water and complex **6**.

Introduction

A principal biological defense against hydrogen peroxide in cells is a class of enzymes called catalases. A relatively new class is the rare dimanganese catalases,[1−3] which disarm peroxide by converting it to water and oxygen (dismutation) at extremely high rates equal to the fastest known enzymatic rate for any biological function.

$$2H_2O_2 \rightarrow 2H_2O + O_2 \quad (1)$$

Catalase mimics have potential biomedical applications as therapeutic agents against oxidative stress. However, so far the best chemical mimics of the dimanganese class of catalases are 10^4−10^5 slower than the enzymes.[4−6] This limitation stems from the lack of complete understanding of the principles of catalysis of peroxide dismutation and therefore is a topic of considerable current interest.

* To whom correspondence should be addressed. E-mail: dismukes@princeton.edu.

(1) Kono, Y.; Fridovich, I. *J. Bacteriol.* **1983**, *155*, 742.
(2) Beyer, W. F.; Fridovich, I. *Biochemistry* **1985**, *24*, 6460.
(3) Barynin, V. V.; Grebenko, A. I. *Dokl. Akad. Nauk. SSSR* **1986**, *286*, 461.
(4) Pecoraro, V. L.; Baldwin, M. J.; Gelasco, A. *Chem. Rev.* **1994**, *94*, 807.
(5) Dismukes, G. C. Manganese Enzymes with Binuclear Active Sites. *Chem. Rev.* **1996**, *96*, 2909.
(6) Wieghardt, K. *Angew. Chem., Int. Ed. Engl.* **1989**, *28*, 1153.

10.1021/ic9911771 CCC: $19.00
Published on Web 06/17/2000

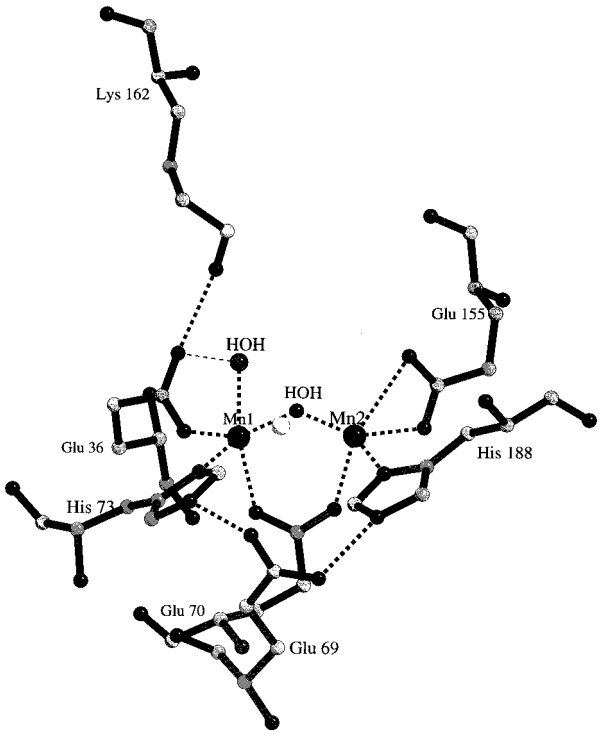

Figure 1. Active site of the reduced form of Mn catalase from *T. thermophilus*. Reprinted with permission of the author.[7]

Structural features of the enzyme are known from a recent X-ray structure diffraction map of the manganese catalase of *T. thermophilus* obtained at 1.4 and 1.6 Å resolution.[7] The enzyme is comprised of six identical subunits (M_r = 35 000 Da/su; su = subunit), and each subunit binds a pair of Mn ions. The binuclear manganese cluster (Figure 1), which is situated in a cavity rich in hydrophobic residues, has a Mn···Mn separation of 3.18 Å in the reduced form, Mn_2(II,II), and 3.14 Å in the oxidized form, Mn_2(III,III). The two Mn ions are bridged by a $\mu_{1,3}$-glutamate residue (Glu70) and two exogenous ligands, which were modeled as a water and hydroxide for the reduced form and as a bridging oxygen and a hydroxide in the oxidized form. A second water molecule bound at a terminal site to Mn1 was observed and identified as a second location for the μ-aqua bridge in 50% of the reduced molecules, thus suggesting an equilibrium for water binding at these two sites (V. Barynin, private communication). Both Mn ions have distorted square pyramidal geometry arising from further coordination to histidine and a second glutamate residue. The Glu36 ligand to Mn1 exists in either bidentate coordination mode (with bridging aqua) or monodentate coordination (with intramolecular hydrogen bonding to a terminal aqua ligand on Mn1). Although the enzyme can exist in at least four different oxidation states,[8] Mn_2(II,II), Mn_2(II,III), Mn_2(III,III), Mn_2(III,IV), it has been shown that the enzyme cycles exclusively between the Mn_2(II,II) and Mn_2(III,III) oxidation states during catalysis.[8−10] Three types of mechanistic proposals[5,10,11] have been suggested that differ according to the geometry of the substrate binding and hence in the HO−OH bond cleavage and electron transfer from HO−OH to Mn_2.

Many manganese complexes encompassing a variety of ligand types and oxidation states have been reported that show catalase activity. The roles of redox state, dinuclearity versus mononuclearity, redox potential, Mn coordination asymmetry, and inner-sphere ligand rearrangements have been explored.[4,12−34] The availability of proton donors/acceptors and the redox-decoupling role of a bridging carboxylate have been found to be important in model complexes and thus have been proposed to be functionally important for the enzymes.[5,35,36] In those few cases where reaction mechanisms have been studied in detail three types of mechanisms have been found that differ primarily in the redox states that are used during catalysis.[12−14,16−18,21−24]

So far only two functional model systems have been proven to use the low-valent Mn_2(II,II) ↔ Mn_2(III,III) cycle similar to the enzyme. Pecoraro et al. obtained a series of structurally characterized six-coordinate Mn_2(II,II) and Mn_2(III,III) complexes derived from a binucleating salen type ligand having a pair of alkoxide bridges that are functional catalase models.[4,14,35,37,38] The complexes exhibit saturation kinetics[14,39] with hydrogen peroxide. The most active of these model complexes has a catalytic efficiency ($(k_{cat}/K_M$ = 990 M^{-1} s^{-1}) that is approximately 575 and 3160 times less effective than the *L.*

(7) Barynin, V. V.; Hempstead, P. D.; Vagin, A. A.; Antonyuk, S. V.; Melik-Adamyan, W. R.; Lamzin, V. S.; Harrison, P. M.; Artymiuk, P. J. *J. Inorg. Biochem.* **1997**, *67*, 196.
(8) Khangulov, S. V.; Barynin, V. V.; Voevodskaya, N. V.; Grebenko, A. I. *Biochim. Biophys. Acta* **1990**, *1020*, 305.
(9) Dismukes, G. C. *Polynuclear Manganese Enzymes*; Reedijk, J., Ed.; Marcel-Dekker: Amsterdam, 1992; p 317.
(10) Penner-Hahn, J. E. *Structural properties of the Mn site in the Mn catalases*; Pecoraro, V. L., Ed.; Verlag Chemie: New York, 1992; p 29.
(11) Meier, A. E.; Whitaker, M. M.; Whitaker, J. W. *Biochemistry* **1996**, *35*, 348.
(12) Pessiki, P. J.; Khangulov, S. V.; Ho, D. M.; Dismukes, G. C. *J. Am. Chem. Soc.* **1994**, *116*, 891.
(13) Pessiki, P. J.; Dismukes, G. C. *J. Am. Chem. Soc.* **1994**, *116*, 898.
(14) Gelasco, A.; Pecoraro, V. L. *J. Am. Chem. Soc.* **1993**, *115*, 7928.
(15) Mathur, P.; Crowder, M.; Dismukes, G. C. *J. Am. Chem. Soc.* **1987**, *109*, 5227.
(16) Larson, B.; Lah, M. S.; Li, X.; Bonadies, J. A.; Pecoraro, V. L. *Inorg. Chem.* **1992**, *31*, 373.
(17) Larson, E. J.; Pecoraro, V. L. *J. Am. Chem. Soc.* **1991**, *113*, 3810.
(18) Larson, E. J.; Pecoraro, V. L. *J. Am. Chem. Soc.* **1991**, *113*, 7809.
(19) Bossek, U.; Saher, M.; Weyhermuller, T.; Wieghardt, K. *J. Chem. Soc., Chem. Commun.* **1992**, 1780.
(20) Sarneski, J. E.; Brzezinski, L. J.; Anderson, B.; Didiuk, M.; Manchanda, R.; Crabtree, R. H.; Brudvig, G. W.; Schulte, G. K. *Inorg. Chem.* **1993**, *32*, 3265.
(21) Sakiyama, H.; Tamaki, H.; Kodera, M.; Matsumoto, N.; Okawa, H. *J. Chem. Soc., Dalton Trans.* **1993**, 591.
(22) Sakiyama, H.; Okawa, H.; Isobe, R. *J. Chem. Soc., , Chem Commun.* **1993**, 882.
(23) Sakiyama, H.; Okawa, H.; Suzuki, M. *J. Chem. Soc., Dalton Trans.* **1993**, 3823.
(24) Gelasco, A.; Askenas, A.; Pecoraro, V. L. *Inorg. Chem.* **1996**, *35*, 1419.
(25) Nagata, T.; Mizukami, J. *J. Chem. Soc., Dalton Trans.* **1995**, 2825.
(26) Nagata, T.; Ikawa, Y.; Maruyama, K. *J. Chem. Soc., Chem. Commun.* **1994**, 471.
(27) Ikawa, Y.; Nagata, T.; Maruyama, K. *Chem. Lett.* **1993**, 1049.
(28) Naruta, Y.; Maruyama, K. *J. Am. Chem. Soc.* **1991**, *113*, 3595.
(29) Naruta, Y.; Sasayama, M. *J. Chem. Soc., Chem. Commun.* **1994**, 2667.
(30) Naruta, Y.; Sasayama, M. *Angew. Chem., Int. Ed. Engl.* **1994**, *33*, 1839.
(31) Devereux, M.; Curran, M.; McCann, M.; Casey, M. T.; McKee, V. *Polyhedron* **1995**, *14*, 2247.
(32) Devereux, M.; Curran, M.; McCann, M.; Casey, M. T.; McKee, V. *Polyhedron* **1996**, *15*, 2029.
(33) Nishida, Y.; Nasu, M. *Inorg. Chim. Acta* **1991**, *190*, 1.
(34) Nishida, Y.; Akamatsu, T.; Tsuchiya, K.; Sakamoto, M. *Polyhedron* **1994**, *13*, 2251.
(35) Pecoraro, V. L.; Gelasco, A.; Baldwin, M. J. *Modeling the chemistry and properties of multinuclear manganese centers*; Kessissoglou, D. P., Ed.; Kluwer Academic Publishers: The Netherlands, 1995; p 287.
(36) Waldo, G. S.; Penner-Hahn, J. E. *Biochemistry* **1995**, *34*, 1507.
(37) Gamelin, D. R.; Kirk, M. L.; Stemmler, T. L.; Pal, S.; Armstrong, W. H.; Penner-Hahn, J. E.; Solomon, E. I. *J. Am. Chem. Soc.* **1994**, *116*, 2392.
(38) Gelasco, A.; Kirk, M. L.; Kampf, J. W.; Pecoraro, V. L. *Inorg. Chem.* **1997**, *36*, 1829.
(39) Gelasco, A.; Bensiek, S.; Pecoraro, V. L. *Inorg. Chem.* **1998**, *37*, 3301.

plantarum[10,40] and *T. thermophilus* enzymes,[41] respectively. Reactions with deuterium peroxide show that proton dissociation/association is important for both complex formation and in the rate-limiting step.[14,35,39]

The other Mn_2(II,II) model system that utilizes the same redox states as the enzyme employs a septadentate ligand with benzimidazolyl groups and a single bridging alkoxide (complexes **1**−**4**).[12,13,15] The Mn(II) ions are five-coordinate, and the most active derivative of this series contains a $\mu_{1,3}$-bridging carboxylato group, $[L^1Mn_2(\mu\text{-OAc})](ClO_4)_2$, (**1**), instead of the six-coordinate derivatives $L^1Mn_2Cl_3$ and $L^1Mn_2(OH)Br_2$.[15] Kinetic and spectroscopic data reveal that the rate-limiting step under steady-state turnover for these reactions is the reduction of hydrogen peroxide by an active Mn_2(II,II) species. This active Mn_2(II,II) species (denoted as $[LMn_2(II,II)(\mu\text{-}O_2CR)]^*$ in eq 2) is formed by reaction of water with the inactive complex **1** during a kinetic lag phase (time required for the onset of O_2 evolution).[12,13]

$$\underset{\text{inactive}}{LMn_2(II,II)(\mu\text{-}O_2CR)} \xrightarrow{H_2O} \underset{\text{active}}{[LMn_2(II,II)(\mu\text{-}O_2CR)]^*} \underset{O_2\ \ H_2O_2}{\overset{H_2O_2\ \ H_2O}{\rightleftharpoons}} LMn_2(III,III)(\mu\text{-}O_2CR)(\mu\text{-}O) \quad (2)$$

The molecular structures of the catalytically active Mn_2(II,II)* and Mn_2(III,III) species in this cycle were not fully determined. Although loss of the kinetic lag phase was shown to occur by reaction with water, it was not established what rearrangement is responsible for activation of the catalyst. Herein we identify the solution-phase molecular structures of the Mn_2(II,II) and Mn_2(III,III) species that are implicated in the catalytic cycle with hydrogen peroxide. Further, the influence on the catalytic rate and substrate affinity of addition of one and two intramolecular hydroxide ligands to the Mn ions has been measured. The kinetic data are correlated with quantitative physicochemical measurements of redox potential and solution structures determined by NMR and EPR experiments.

Experimental Section

Reagents. See the Experimental Section of ref 42. All solvents were of analytical grade and used without further purification unless stated otherwise. $[L^1Mn_2(CH_3CO_2)](ClO_4)_2$ (**1**) and $[L^1Mn_2(ClCH_2CO_2)](ClO_4)_2$ (**2**), where L^1 is *N*,*N*,*N*′,*N*′-tetrakis(2-methylenebenzamidazolyl)-1,3-diaminopropan-2-ol, were synthesized as described previously.[12] *N*,*N*,*N*′,*N*′-tetrakis(2-(1-ethylbenzamidazolyl))-2-hydroxy-1,3-diaminopropane (L^2) was synthesized according to the procedure of McKee et al.[43] The dimanganese(II,II) complexes $[L^2Mn_2(CH_3CO_2)](ClO_4)_2$ (**3**) and $[L^2Mn_2(ClCH_2CO_2)](ClO_4)_2$ (**4**) were prepared as described before[42] and isolated as white crystalline solids. Further details on the characterization of complexes **6**−**8** can be found in the preceding paper. The abbreviations L^1 and L^2 in complex formulas denote the deprotonated ligands that form a μ-alkoxide bridge between the two manganese ions.

In situ Conversion of Complexes 1 and 3 to Complex Type 7A. To 1×10^{-2} mmol of **1** or **3** dissolved (complex **1**) or suspended (complex **3**) in 1 mL of methanol was added 1×10^{-2} mmol NaOH under argon.

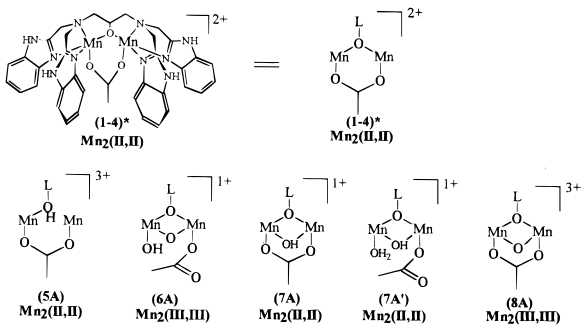

Figure 2. Structures of the species discussed in the text. For complexes **1** and **2**, the ligand is L^1 = *N*,*N*,*N*′,*N*′-tetrakis(2-methylenebenzamidazolyl)-1,3-diaminopropan-2-ol. For complexes **3** and **4**, the ligand is L^2 = *N*,*N*,*N*′,*N*′-tetrakis(2-(1-ethylbenzamidazolyl))-2-hydroxy-1,3-diaminopropane.

In situ Conversion of Complexes 1 and 3 to Complex Type 7B. To 1×10^{-2} mmol of **1** or **3** dissolved (complex **1**) or suspended (complex **3**) in 1 mL of methanol was added 5×10^{-2} mmol of NaOH under argon.

In situ Conversion of Complexes 1 and 3 to Complex Type 8. To 1×10^{-2} mmol of **1** or **3** dissolved (complex **1**) or suspended (complex **3**) in 1 mL of methanol was added 2×10^{-2} mmol of NaOH under air. For both cases, an immediate change was observed from colorless to bright-orange.

In situ Conversion of Complexes 1 and 3 to Complex Type 6. To 1×10^{-2} mmol of **1** or **3** dissolved (complex **1**) or suspended (complex **3**) in 1 mL of methanol was added 5×10^{-2} mmol NaOH under air. For both cases, an immediate change was observed from colorless to bright-orange.

Physical Measurements. Equipment and experimental conditions for optical spectroscopy, NMR, EPR, mass spectroscopy, and electrochemistry were all discussed previously.[42]

Oxygen Detection. The time course of oxygen concentration[44] was determined amperometrically using a Clark-type Pt electrode (YSI Yellow Springs), which is covered by a Teflon membrane. All reactions were done as described before,[13] anaerobically in methanol or in water/methanol mixtures that were degassed by argon. The order of addition of reactants had no consequence on the measured rate of oxygen production. The hydrogen peroxide solutions were made from 30% aqueous solutions diluted in methanol (concentration was verified by absorption at 230 nm using $\epsilon = 60\ cm^{-1}$).

Results

Catalase Activity of Complexes 1, 3, 7A, and 7B. An initial lag phase (i.e., the time required for the onset of O_2 evolution) for the catalase activity starting with complex **1** was previously reported by Pessiki et al. (see Figure 2 of this paper and Scheme 3 in the preceding article for molecular formulas).[13] This lag phase was shown to decrease, and the steady-state rate was shown to increase by 5- to 6-fold upon preequilibration with water, hypothesized to represent dissociation of the μ-acetate, since addition of an excess of acetate increased the lag phase and slowed the steady-state catalase rate. However, the lag phase could never be eliminated completely because addition of more than 2% of water slowed the steady-state catalase rate and did not decrease the lag phase any further.

Figure 3 shows that addition of NaOH to a methanolic solution of complex **1** prior to the addition of H_2O_2 eliminates the lag phase completely and increases the steady-state O_2 evolution rate. This rate increases linearly by 93-fold between 0 and 5 equiv of NaOH at which an end point is reached with only an additional 6% increase upon further addition of up to

(40) Waldo, G. S.; Yu, S.; Penner-Hahn, J. E. *J. Am. Chem. Soc.* **1992**, *114*, 5869.
(41) Shank, M.; Barynin, V.; Dismukes, G. C. *Biochemistry* **1994**, *33*, 15433.
(42) Boelrijk, A. E. M.; Khangulov, S. V.; Dismukes, G. C. *Inorg. Chem.* **2000**, *39*, 3009.
(43) McKee, V.; Zvagulis, M.; Dagdigian, J. V.; Patch, M. G.; Reed, C. A. *J. Am. Chem. Soc.* **1984**, *106*, 4765.
(44) Battino, R., Ed. *Oxygen and Ozone*; Solubility Data Series 7; Pergamon Press: New York, 1981.

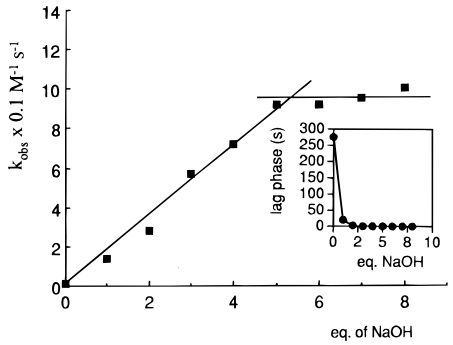

Figure 3. Increase of k_{obs} for the catalase reaction of **1** in methanol upon addition of NaOH, from 0 equiv (k_{obs} is 1.0 M^{-1} s^{-1}) to 8 equiv (k_{obs} is 100 M^{-1} s^{-1}) of NaOH. The inset shows the decrease in lag phase upon addition of NaOH. See text for details.

8 equiv of NaOH. All necessary blanks were done to prove that neither hydroxide itself nor the free ligand is responsible for this effect (spontaneous dismutation). In the inset of Figure 3, the duration of the lag phase is shown to be essentially eliminated by addition of only 1 equiv of NaOH. The stoichiometric conversion is consistent with formation of a new species for which electrochemical evidence supports the formulation $[LMn_2(II,II)(\mu\text{-OH})(\mu_{1,3}\text{-OAc})]^+$, complex **7A**.[42]

The rate expression that was previously established under nonsaturation conditions of substrate,[13]

$$\frac{d[O_2]}{dt} = k_{obs}[H_2O_2]^1[\text{complex } \mathbf{1}]^1 \qquad (3)$$

was used to evaluate the rate constant. Using the steady-state oxygen evolution rate (after the lag phase), we calculate the observed rate constant (k_{obs}) to increase linearly from 1.0 M^{-1} s^{-1} (at 0 equiv of NaOH) to 92 M^{-1} s^{-1} (at 5 equiv of NaOH) and 100 M^{-1} s^{-1} (at 8 equiv of NaOH). The H_2O_2 dismutation reaction catalyzed by complex **3** (the N-ethylated analogue of **1**) was accelerated by NaOH in the same manner as complex **1**, i.e., with a breakpoint in the rate acceleration between 4 and 5 equiv of NaOH, a k_{obs} of 8.5 M^{-1} s^{-1} at 0 equiv (lag phase 450 s) and 291 M^{-1} s^{-1} at 5 equiv of NaOH. Moreover, the lag phase is also eliminated after only 1 equiv of NaOH, consistent with formation of a new species $[L^2Mn_2(II,II)(\mu\text{-OH})(\mu_{1,3}\text{-OAc})]^+$ analogous to the behavior of complex **1**. We conclude therefore that the rate acceleration and loss of lag phase cannot be related to deprotonation of the benzimidazole groups on the ligand. The fact that the addition of water to complex **1** can also decrease the lag phase (up to 50%) suggests that some μ-hydroxo-bridged $Mn_2(II,II)$ dimer, species **7A**, is produced by hydrolysis. On the basis of these rate data and EPR data showing formation of an uncoupled Mn(II) species,[13,42] we conclude that spontaneous deprotonation of the μ-aqua ligand in $[LMn_2(II,II)(\mu\text{-}H_2O)(\mu\text{-OAc})]^{2+}$, complexes **1**−**4**, yields approximately equal amounts of the (catalytically active) deprotonated μ-hydroxide species $[LMn_2(II,II)(\mu\text{-OH})(\mu\text{-OAc})]^{1+}$, complex **7A**, and the (inactive) protonated complex **5A**, $[LHMn_2(II,II)(\mu\text{-}H_2O)(\mu\text{-OAc})]^{3+}$, containing the neutral ligand (LH) with a protonated alkoxide group (alcohol). Complex **5A** is observed by EPR to be a spin-uncoupled Mn(II) species that retains both Mn(II) ions.[13,42] We observed no evidence that linked catalytic activity to the presence of the spin-uncoupled $Mn(II)_2$ species, complex **5**. Uncoupling of the Mn(II) ions by protonation of the ligand (LH) leads to lower catalase activity.

When the concentrations of H_2O_2, complex **1**, and NaOH (at 5 equiv) are held constant, the rate of O_2 evolution was measured as a function of water concentration. Contrary to the previous results on complex **1** without NaOH that indicated a *decrease* of k_{obs} with increasing water content above 2% in methanol,[13] the present data for **1** with 5 equiv of NaOH show an *increase* in k_{obs} from 9.2 M^{-1} s^{-1} (in 98/2 v/v methanol/water) to 24.8 M s^{-1} (in 11/89 v/v methanol/water). We tentatively attribute this increase in rate upon increase of water content in the solvent to an enhanced rate of proton exchange relative to methanol solvent between H_2O_2 and the catalyst during the peroxide dismutation.

In contrast to NaOH, the addition of 0−5 equiv of the noncoordinating base 2,6-di(tertbutyl)pyridine (TBP) to complexes **1**−**4** does not change the steady-state oxygen evolution rate or the lag phase. TBP was found[42] to affect the electrochemical potential for the redox couple $Mn_2(III,III)/(III,IV)$ but not the couple $Mn_2(II,II)/(III,III)$, indicating that the $Mn_2(III,IV)$ state is not involved in the catalase activity. This result supports earlier conclusions.[13]

We also conclude that the role of hydroxide is more than merely to act as an outer-sphere (uncoordinated) base, since TBP (a noncoordinating base) has no effect whatsoever. Instead, the function of hydroxide is linked to its ability to bind to one or both of the Mn ions. Therefore, an intramolecular base is indicated for catalysis.

Characterization of the Active Species in the Catalytic Cycle. Previously,[42] we demonstrated the utility of NMR spectroscopy to monitor the change in coordination mode of the acetate group to the oxidized $Mn_2(III,III)$ species, **6** vs **8**. Hence, this method also was used under catalytic conditions in the presence of H_2O_2. EPR measurements under these conditions did not yield useful information because the catalyst occurs in the $Mn_2(III,III)$ state under catalytic conditions and the ground state is diamagnetic. A 10 mM sample of complex **8** in CD_3OD was obtained in situ by adding 1 equiv of NaOH to a 10 mM solution of complex **3** in CD_3OD under aerobic conditions, as described in the Experimental Section. Either a 10-fold or 20-fold excess of hydrogen peroxide was added to two samples of complex **8** in which the $\mu_{1,3}$-bridging acetate is present and easily monitored by a broad signal at 22.8 ppm.[42] Immediately after addition of the hydrogen peroxide, oxygen bubbles are observed and the broad resonance at 22.8 ppm starts disappearing, while the resonance associated with monodentate bound acetate at 1.9 ppm increases proportionally at the same time (Figure 4). The proton resonances from the ligand remain unchanged, which indicates that the complex is stable under catalytic conditions. Addition of more H_2O_2 to the sample produced more dioxygen evolution but did not further change the NMR spectrum. After more than 2000 turnovers no evidence of ligand or catalyst decomposition was observed.[13] The NMR spectrum obtained after reaction of **8** with 10 or 20 equiv of H_2O_2 is identical to the NMR spectrum of an authentic sample of complex **6** in CD_3OD, which was obtained from complex **3** upon addition of 4−5 equiv of NaOH, as described in detail before.[42] From this experiment we conclude that $Mn_2(III,III)$ species **6**, possessing a monodentate acetate and a terminal OH^-, is formed at the end of the catalytic disproportionation reaction with hydrogen peroxide. The UV−vis spectrum of **6** in methanol was reported before[42] and is identical to the spectrum of the reaction intermediate obtained upon reaction of complex **1** with a stoichiometric amount of H_2O_2 in methanol.[13] Both spectra reveal three absorption peaks at 425, 472, and 760 nm, which are consistent with oxidation to a Mn(III) or $Mn_2(III,III)$ species. A linear correlation is found between the concentration of **6** in solution (as measured by UV−vis spectroscopy) and the catalase

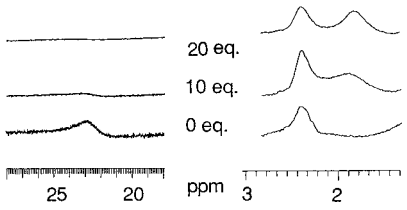

Figure 4. ^{1}H NMR spectra showing the appearance of absorption peaks of derivative **6** upon addition of 10 and 20 equiv of H_2O_2 to species **8**. The decreasing signal at 22.8 ppm is the methyl group of $\mu_{1,3}$-bridging acetate. The increasing signal at 1.9 ppm is of the methyl group of monodentate coordinated acetate, and the signal at 2.45 ppm is from ligand L[2]. For further details for assignment of signals, see the preceding article.

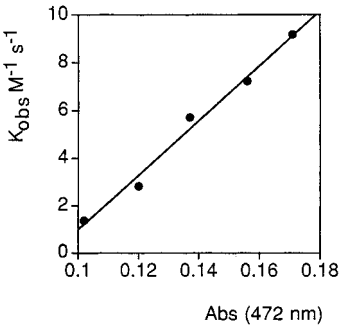

Figure 5. Correlation between the concentration of complex **6** in solution as measured by its absorption at 472 nm and the k_{obs} of the catalase reaction (solvent is methanol).

rate observed for this solution (Figure 5). Therefore, we conclude that complex **6** is the oxidized form of the active catalyst under multiple turnover conditions.

A nonbridging carboxylate, e.g., in the form of a monodentate coordinated acetate, is not a prerequisite for an active catalyst, as seen by the loss of the kinetic lag phase upon coordination of hydroxide to complex **1** in forming LMn_2(II,II)(μ-OH)(μ-O_2CCH_3), complex **7A**. NMR reveals that after oxidation by H_2O_2 of complex **7A** the symmetrical bridging acetate is converted to a monodentate coordinated acetate in the Mn_2(III,III)(μ-O) species, complex **6**. Upon rereduction of complex **6** with hydrogen peroxide, the terminal carboxylate need not rebridge, forming LMn_2(II,II)(μ-OH)(O_2CCH_3)(H_2O), complex **7A′**, which would be in equilibrium with complex **7A** by dissociation of water upon a carboxylate shift to the bridging position. Thus, the μ-hydroxide appears to increase the lability of the bridging carboxylate in the reduced complexes (**7A′**/**7A**). This interconversion of species (**7A′**/7A) is included in the catalytic cycle under steady-state turnover conditions (Scheme 2). Although these intermediates have been identified in solution using spectroscopic methods, further support could be sought from single turnover experiments with 1 equiv of H_2O_2 and the isolated complexes **6** and **7A**/**7A′**. However, so far we were unable to isolate these intermediates as homogeneous solids that would be suitable for these kinds of experiments.

An additional feature of the NMR spectrum of the oxidized derivatives **8** and **6** obtained by alkaline oxidation in air of complex **1** compared to the spectra of derivatives **8′** and **6′** obtained by oxidation of complex **3** is the presence of six partly overlapping broad signals in the 10−30 ppm region, which were assigned to protons on the benzimidazole nitrogens.[42] Since there are only four NH groups in complex **1**, the existence of six different N−H signals indicates the presence of more than one species. However, when the freshly oxidized sample is left for 1 h at room temperature, the NMR spectrum simplifies to a new spectrum expected for a symmetric (μ-O)−(μ-OR)-Mn_2(III,III) species in which only two NH groups are detected at 12 and 17 ppm with equal relative areas.[42] This conversion in the N−H region of the spectrum can also be accomplished instantaneously by adding hydrogen peroxide. This result indicates that under catalytic conditions only one Mn_2(III,III) species is present that has two pairs of inequivalent N−H

Scheme 1. Proposed Mechanism[5] for Mn Catalase

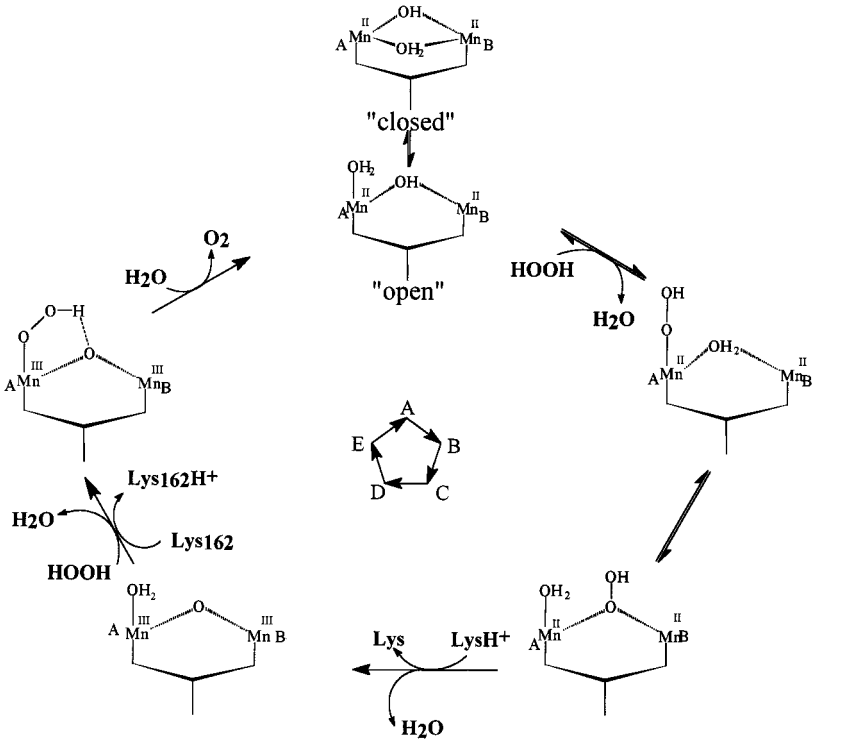

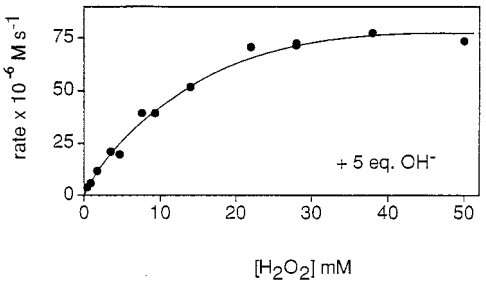

Figure 6. Saturation kinetics for the hydrogen peroxide disproportionation reaction for complex **1** in methanol upon addition of 5 equiv of NaOH prior to the reaction. Oxygen evolution rate is measured as a function of the hydrogen peroxide concentration in solution.

protons. In addition, the latter spectrum does not contain a $\mu_{1,3}$-acetate signal at 22.8 ppm but has instead a signal at 1.90 ppm due to a monodentate acetate, indicating that the acetate bridge is broken during catalytic turnover. The proposed structure for complex **6** (Figure 2) with terminal acetate bound to one of the Mn(III) ions is consistent with these results. Thus, complex **6** forms both during catalytic turnover with H_2O_2 and upon air oxidation in the presence of 2 equiv or more of base. We imagine that complex **6** may be in equilibrium with complex **8** in aqueous solvents where displacement of hydroxide would be assisted by protonation. We attribute the conversion of **6** to **8** with the modest rate increase seen upon addition of water.

Substrate Saturation Kinetics. The dependence of the steady-state kinetics of H_2O_2 consumption on initial H_2O_2 concentration was determined as O_2 evolution in 98% MeOH/2% water for complex **1** with 0, 1, and 5 equiv of NaOH (Table 1, Figure 6A, and Supporting Information) and at 9-fold greater water concentration (89% H_2O/11% MeOH with 5 equiv of NaOH; Table 1 and Supporting Information). These latter experiments were performed to learn if water solvation might influence the rate parameters. The kinetic data establish that saturation of the rate occurs with increasing H_2O_2 concentration. Also, the dependence on the catalyst concentration is linear over the range 0.1−4 mM (data not shown). Table 1 summarizes the steady-state rate parameters (k_{cat} and K_m) obtained from Lineweaver−Burke plots (reciprocal rate^{-1} vs $[H_2O_2]^{-1}$, not shown). Steady-state kinetic data were obtained after the lag phase.

For complex **1** without hydroxide added, a K_m of 35 ± 8 mM is determined, which compares to a K_m of 10 mM for the [Mn(III)(2-OHsalpn)]$_2$ model[39] and 83 and 15 mM for the MnCat's from *T. thermophilus*[41] and *T. album*,[10] respectively. By contrast, the k_{cat} of **1** is 0.1 s^{-1}, which is smaller by 100, or 2.6×10^6 and 2.6×10^5 times that found for the salpn dimer[39] MnCat from *T. thermophilus*[41] and MnCat from *T. album*,[10] respectively. As a consequence, the catalytic efficiency (k_{cat}/K_M) of complex **1** is 10^5-10^6 lower than the catalase enzymes from these organisms. Upon addition of 1 equiv of hydroxide to **1**, forming complex **7A**, the K_m for peroxide disproportionation decreases 5-fold from 35 ± 8 to 7 ± 2 mM, while the k_{cat} increases 6.5-fold from 0.1 to 0.65 s^{-1}, resulting in a 32-fold increase in catalytic efficiency. We propose that the lower Michaelis constant (K_m) for the μ-hydroxide species **7A** could be due to a higher affinity for binding of the hydroperoxyl anion (HO_2^-) vs binding of hydrogen peroxide to **1**. Thus, the catalytic function of the μ-hydroxide appears to include deprotonation of the substrate by ligand exchange into the bridging position:

$$\mu\text{-}OH^- + H_2O_2 \rightarrow \mu\text{-}O_2H^- + H_2O \qquad (4)$$

Scheme 2. Proposed Dismutation Mechanism for the Hydroxide Derivatives of Complex **1**

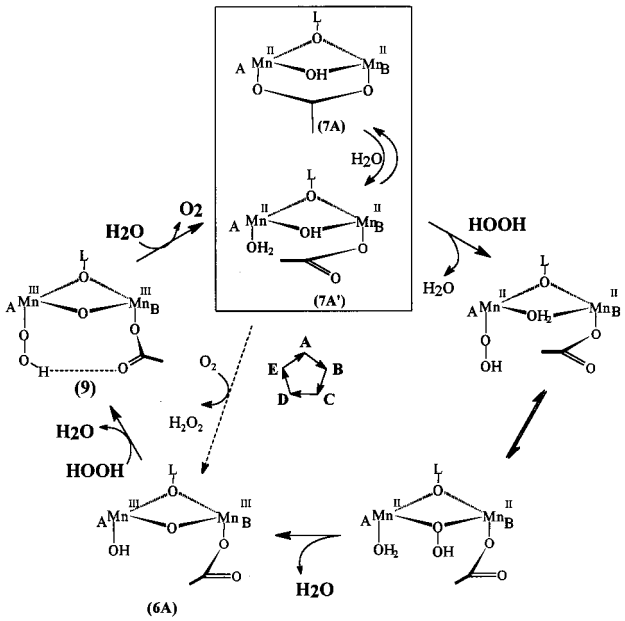

The fact that noncoordinating bases such as 2,6-di(*tert*-butyl)-pyridine (TBP) have no effect on either the K_m or k_{cat} of the peroxide dismutation reaction with complex **1** supports this proposal and establishes convincingly that bound hydroxide and not free base in solution is responsible for the enhanced catalase rate. Several lines of evidence establish coordination of hydroxide to complex **1**, forming complex **7A**, including the loss of the steady-state kinetic lag phase, EPR, FTIR, and cyclic voltammetry data.[42] Since the rate-determining step in the H_2O_2 disproportionation cycle is the oxidation to a Mn_2(III,III) species from Mn_2(II,II), the 6.5-fold increase in k_{cat} could be explained if there is a lower activation energy barrier to the oxidation step. Voltammetry data show a considerably easier oxidation potential for the bridging hydroxide complex **7A** versus the hydroxide-free complexes **1**−**4**.[42] Previous work has also shown that bridging OH^- facilitates oxidation in the related Mn_2(II,II) complexes $[LMn_2(\mu\text{-}X)Y_2]^{2+}$ (X = Cl or OH^-, Y = Cl^- or Br^-) that lack carboxylate.[15]

The lack of further change in the K_m when two to five hydroxides are added to the medium (Table 1) indicates that the binding affinity of the initial substrate (hydroperoxide) that is monitored in the steady-state kinetic experiment is not further altered by excess hydroxide. Because we found no evidence for a change in which of the two redox steps is the slowest with excess hydroxide concentrations—it remains oxidation of the Mn_2(II,II) precursor species rather than reduction to Mn_2(II,II)—we may conclude that only the steps leading to formation of this reduced precursor may contribute to increasing the catalyst's binding affinity for the initial substrate molecule (so-called Michaelis complex).[52] These steps correspond to steps

(45) Khangulov, S. V.; Goldfeld, M. G.; Gerasimenko, V. V.; Andreeva, N. E.; Barynin, V. V.; Grebenko, A. I. *J. Inorg. Biochem.* **1990**, *40*, 279.
(46) Shank, M. Unpublished data.
(47) Stenkamp, R. E.; Sieker, C.; Jensen, L. H.; McCallum, J. D.; Sanders-Loehr, J. *Proc. Natl. Acad. Sci. U.S.A.* **1985**, *82*, 713.
(48) Khangulov, S. V.; Pessiki, P. J.; Barynin, V. V.; Ash, D.; Dismukes, G. C. *Biochemistry* **1995**, *34*, 2015.
(49) Manchandra, R.; Brudvig, G. W.; Crabtree, R. H. *Coord. Chem. Rev.* **1995**, *144*, 1.
(50) Rardin, R. L.; Tolman, W. B.; Lippard, S. J. *New. J. Chem.* **1991**, *15*, 417.

Table 1. Steady-State Kinetic Parameters of Complex **1** under Different Conditions and Comparison with Catalase Enzymes and Catalase Mimics

catalyst	ref	K_m (mM)	k_{cat} (s^{-1})	k_{cat}/K_m (s^{-1} M^{-1})
1[a]	this work	35 ±15	0.1 ± 0.005	2.9
1[a] + 1 equiv OH^- (**7A**)	this work	7 ± 3	0.65 ± 0.05	92
1[a] + 5 equiv OH^- (**6**)	this work	6 ± 4	2.7 ± 0.1	450
1[b] + 5 equiv OH^- (**6**)	this work	0.3 ± 0.04	2.1 ± 0.1	700
$[Mn^{III}(2\text{-OHsalpn})]_2$	39	10.2 ± 0.4	10.1 ±0.2	990
$[Mn_2II(^2L)(PhCO_2)_2(NCS)$[c]	21−23	nd	$k_{obs} = 0.33\ M^{-1}\ s^{-1}$	nd
MnCat (*T. thermophilus*)	41	83 ± 8	2.6×10^5	3.13×10^6
MnCat (*L. plantarum*)	10, 41	350	2.0×10^5	0.57×10^6
MnCat (*T. album*)	2	15	2.6×10^4	1.73×10^6

[a] Complex **1** in 98% methanol/2% water. [b] Complex **1** in 89% water/11% methanol. [c] ^{2}L is 2,6-bis[*N*-((2-dimethylamino)ethyl)amino)methyl-4-methylphenolate (**1**−). Saturation kinetics were not demonstrated nor was the molecularity of the reaction established. The number given represents the reported rate divided by the concentrations of catalyst and peroxide.

A → B → C in Scheme 2 in which the substrate binds as the μ-hydroperoxide to **7A′** by exchange with the hydroxide bridge: μ-$OH^- + H_2O_2 \rightarrow \mu$-$O_2H^- + H_2O$. Subsequent steps (D → E) that follow formation of the oxidized complex **6A** and precede its reduction (E → A) do not contribute to the affinity of the Michaelis complex and therefore do not show up in the K_m.

The kinetic data also show that k_{cat} increases 4-fold with no change in K_m upon addition of 2−5 equiv of hydroxide (Table 1). This result is consistent with the model described above in which substrate binding to the oxidized complex **6A** or reduction to **7A′** is accelerated by excess hydroxide, but neither is rate-limiting in the steady-state. We suggest that the step that is accelerated by excess hydroxide may involve the reduction of complex **6A** to form complex **9** (step D → E), as depicted in Scheme 2. This suggestion is based on the electrochemical data showing that the electrochemical potential for reduction of the oxidized Mn_2(III,III) species is greater upon binding of a second hydroxide, and thus, a greater driving force for reduction exists (Scheme 1 of ref 42). Direct evidence for the formation of complex **6A** by air oxidation of **7** in alkaline solutions was previously demonstrated,[42] and this species was found to be immediately active in the catalase reaction with added peroxide with no lag-time observed (data not shown).

These mechanistic conclusions are confirmed in other examples of "ping−pong" kinetics involving conversion of two substrate molecules in sequential steps by an enzyme (E_0) or catalyst following preequilibrium binding.[52] The steady-state expression for the transit time, eq 5,[52] the time required for 1 mol of substrate to pass through all steps in the mechanism given in Scheme 2, can be reduced to a sum of four terms:

$$\frac{[E_0]}{v} \equiv \frac{K_m}{k_{ox}[H_2O_2]} + \frac{1}{k_{ox}} + \frac{K_m'}{k_{red}[H_2O_2]} + \frac{1}{k_{red}} \qquad (5)$$

The first term involves the time for initial substrate binding (steps A → B → C) governed by the Michaelis constant for the reduced precursor (K_m); the second term involves the time required for irreversible oxidation of this precursor complex (step C → D); the third term involves the time required for substrate binding to the oxidized catalyst (step D → E) governed by the Michaelis constant for the oxidized catalyst (K_m'); and the last term is the time for regeneration of the reduced catalyst by the second substrate molecule (step E → A). Since we observe that oxidation of the catalyst is always the slower of the two redox steps for all hydroxide concentrations ($k_{ox} \ll k_{red}$), we may safely conclude that the first two terms will dominate in the transit time and that the first term will make the dominant contribution to the observable Michaelis constant. Thus, one or more of the initial binding steps A → B → C provide the major contribution to the rate acceleration/affinity increase seen upon addition of the first hydroxide, while excess hydroxides appear to contribute principally to the rate of the reduction step (D → E).

When the water content of the solvent system is increased by 9-fold to 89%, the K_m decreases further from 6 ± 2 mM to 0.3 ± 0.02 mM (both measured with 5 equiv of NaOH plus complex **1**; Figure 7 and Table 1**)**. Little change occurs in the k_{cat} with water content. A catalyst efficiency (k_{cat}/K_M) of 700 s^{-1} M^{-1} is observed that is only 800 times slower than the efficiency of MnCat from *L. plantarum* (see Table 1). Upon addition of more than 1.5 mM hydrogen peroxide (>5-fold above the K_m), the reaction rate increases again in a linear fashion above its initial saturation plateau and no new saturation level is observed. This result indicates that a new catalase mechanism of lower efficiency can also be observed at very high substrate concentrations but only in the presence of high water content in the solvent. We have not explored the rate parameters associated with this new mechanism. The following discussion focuses on the mechanism observed in 98% methanol/2% water.

General Discussion

Several mechanisms for the hydrogen peroxide dismutation reaction by catalases have been proposed.[5,10,11] The mechanism that we and others have investigated in the case of the *T. thermophilus* enzyme is given in Scheme 1,[5] which is based on both the available enzymological data and the most recent X-ray structural data[7] for the reduced Mn_2(II,II) form and the air-oxidized Mn_2(III,III) form at 1.6 Å resolution. The active site of the enzyme (Figure 1) was found to consist of two major conformers in equal population, a "closed" form with two bridging solvent ligands formulated as (μ-OH)(μ-OH_2), and an "open" form with a single bridge (μ-OH) and a terminal aqua ligand on Mn_A. In the first step of the proposed enzymatic reaction (Scheme 1, A → B) hydrogen peroxide binds to the "open" form as a terminal hydroperoxide anion to the five-coordinate Mn_A(II) by releasing the water ligand. This step is coupled to transfer of a substrate proton to a nearby base, which was proposed to be the μ-OH bridge, forming μ-aqua. In the next step (B → C) this neutral μ-aqua bridge exchanges sites with the anionic terminal hydroperoxide (yielding μ-η_2-OOH^-), driven by the more favorable charge neutralization for bridging vs terminal anions, as demonstrated for the case of μ-OH^- by the present complexes **1**−**4**.[42] Anion binding studies to *T.*

(51) Barynin, V. Personal communication, 1997.
(52) Fersht, A. *Enzyme Structure and Mechanism*; W. H. Freeman: New York, 1985; p 115.

thermophilus catalase also demonstrate that various monoanions prefer to bind in the bridging site.[45,46] Therefore, the hydroperoxide anion was also proposed to undergo a critical step in which it exchanges sites from a terminal to bridging μ-η^2-hydroperoxide. The next step (C → D) was proposed to be the cleavage of the hydroperoxide O−OH bond to give μ-oxo and a water molecule. This step was proposed to be driven by concerted protonation of the nonbridging hydroxyl group of the hydroperoxide anion coupled to transfer of two electrons from the Mn(II) ions to give the Mn_2(III,III) oxidation state. This oxidation step is known to be the slower of the two redox transitions in the steady state with excess substrate. Although the identity of this internal proton donor is not fully established, the proximity of Lys162(H^+) (hydrogen-bonded to the Glu36 ligand to Mn_A) and the measured pK_A = 10.5 for the functional proton donor in catalysis[45] would be consistent with Lys162(H^+) functioning in this role. The remaining steps in the catalytic cycle are not rate-limiting and have not been well characterized experimentally. It was suggested that the terminal water ligand to Mn_A of the Mn_2(III,III) intermediate D occupies the likely site for binding of the second substrate molecule following intramolecular deprotonation to form the terminal hydroperoxide in a reaction that may involve Lys162 serving as the base (step D → E). We will show kinetic data for complex **6**, which support this step as a possibility for the enzyme. We anticipate that the terminal hydroperoxide ligand could be stabilized by intramolecular hydrogen-bonding to μ-oxo in intermediate E. The binding of HOO^- in species E as a terminal ligand that is hydrogen-bonded to the μ-oxo is based on the analogous structure found for oxyhemerythrin where a diiron(II,II)(μ-OH) core binds[47] molecular O_2. In the final step (E → A), O_2 is released by concerted transfer of the proton (to μ-oxo) and two electrons from peroxide to reduce Mn_2(III,III) and restore the reduced Mn_2(II,II)(μ-OH) "open" species.

Scheme 2 summarizes our proposed mechanism for peroxide dismutation catalyzed by the hydroxide derivatives of complexes **1** and **3** based on work reported herein and the preceding article.[42] It was shown in the preceding article[42] that under anaerobic conditions addition of 1 equiv of NaOH to complex **1** forms complex **7A**, while under aerobic conditions oxidation to complex **8A** occurs. Addition of more than 3 equiv of NaOH to complex **1** forms complex **7A′** under anaerobic conditions, while oxidation to complex **6A** occurs under aerobic conditions. Both in complexes **7A′** and **6A** the bridging acetate is converted to a monodentate bound acetate upon aquation of the μ-hydroxo (or μ-oxo) species while preserving a maximum coordination number of 6.

The peroxide dismutation mechanism in Scheme 2 differs from the mechanism of the aqua derivatives of complex **1** that was proposed previously.[13] We start in Scheme 2A with the μ-OH bridged complex **7A**. This structure is analogous to the "closed" form of MnCat(II,II) described by X-ray crystallography above (Scheme 1) because all six coordination sites on both Mn(II) ions are occupied. Species **7A** has two six-coordinate Mn(II) ions with three μ-bridging anions and appears to be in equilibrium with a ring-opened form having terminal OAc^- and water molecule (species **7A′**), based on the ligand exchange equilibria[42] and on known model complexes of Mn_2(II,II).[48,49] Hence, species **7A** is expected to be kinetically accessible via the hydrated species **7A′**. Species **7A**/**7A′** with a μ-OH bridge also has a two-electron Mn_2(II,II) ⇔ Mn_2(III,III) redox gap that is 730 mV smaller relative to the parent complex **1** (lacking μ-OH bridge) and consequently has a lower activation barrier to oxidation. The 10-fold increase in the rate constant k_{obs} for the steady-state peroxide dismutation reaction observed with species **7A** or **7A′** vs species **1** and **3** could be partly or entirely due to this decrease in redox potential.

In order for this proposal to be correct, the rate-limiting step in the reaction with H_2O_2 must also involve oxidation of complex **7A** or **7A′** to a Mn_2(III,III) species such as complex **6A**. In step A → B, binding of hydrogen peroxide to species **7A** by displacement of a water ligand is proposed to be facilitated by the hydroxide bridge, which acts as a base to deprotonate H_2O_2. In step B → C the terminal HO_2^- anion in B should migrate to the bridging position to form a μ,η_2 hydroperoxide bridge by exchange with μ-aqua. This exchange would be driven by the strong thermodynamic preference for anions to bind at the bridging site between the metal cations.[15,42,48] Peroxide bridging by displacement of μ-aqua is expected to be coupled to weakening of the acetate affinity, thus forming a monodentate acetate on the free Mn site, which lacks the water ligand, e.g., a carboxylate shift.[50] Conversion of μ-acetate to terminal acetate is reasonable by analogy to the observed conversion of μ-acetate to labile terminal acetate upon treatment of species **7A** with more than 2 equiv of hydroxide.[42]

In the next step (C → D, Scheme 2), bond cleavage of the hydroperoxide is proposed by coupling protonation of the terminal hydroperoxide with Mn_2(II,II) oxidation to yield the (μ-O)-Mn_2(III,III) species, complex **6A**, and free water. This step is analogous to the enzyme mechanism but employs a stereochemically awkward weak proton donor, a water molecule coordinated at a gauche position relative to the position of the hydroperoxide, which is likely to require an additional proton shuttle group such as a solvent water molecule to facilitate proton transfer to the terminal site of the hydroperoxide. In the enzyme a protein side chain (Lys162H^+) may facilitate this step.[51] The resulting Mn_2(III,III) species in D was shown to be accessible by air oxidation of **7A** (see shunt pathway). Similar chemistry appears to describe the air-induced oxidation of MnCat(II,II) to MnCat(III,III) in base.[8,9]

The next step (D → E) of the mechanism is proposed to involve binding and deprotonation of the second substrate molecule by the bound hydroxide to yield a terminally bound hydroperoxide anion species **9** and release of a water molecule. Our kinetic evidence indicates that this second hydroxide binds more weakly then the first one, requiring 5 equiv of NaOH in solution to saturate binding and accelerating the observed rate by an additional 4-fold without affecting K_m (Table 1). We hypothesize that intermediate E may be stabilized by intramolecular H-bonding between the terminal hydroperoxide and the juxtaposed terminal acetate, although we have no structural evidence for this suggestion. Intermediate E may also be stabilized by intramolecular H-bonding between the terminal hydroperoxide and the μ-O^{2-} (as was previously proposed for catalase; see Scheme 1). Intramolecular H-bonding would facilitate the final step E → A involving coupled deprotonation and two-electron oxidation of the hydroperoxide to re-form the starting species (**7A**/**7A′** and release of the product O_2 molecule, thus completing the catalytic cycle.

It has been proposed that the alkoxide bridge of the salpn ligand serves as an internal base in the $Mn(III)_2$(2-X(5-Y)salpn)$_2$ (X = OH or H, Y = Cl or H) complexes,[35,39] which are another class of complexes for which saturation kinetics for the H_2O_2 disproportionation reaction has been reported.[14,39] The data presented herein indicate that the hydroxide ligand in complex **7A** or **7A′** serves as the intramolecular base in preference to the alkoxide. This hydroxide ligand increases the affinity by 5-fold for coordination of H_2O_2 in step A → B (Scheme 2) and

results in a Michaelis constant K_m that is similar or lower than those observed for the $Mn(III)_2(2\text{-}X(5\text{-}Y)salpn)_2$ (X = OH or H, Y = Cl or H) complexes (Table 1). The unimolecular catalytic rate constant k_{cat} obtained for the complexes **1**, **7A**/**7A′** and **6A** are lower, between 42- and 219-fold (complex **1**), between 6.5- and 34-fold (complex **7A**), between 1.5- and 8-fold (complex **6** in 98% methanol), and between 20- and 104-fold (complex **6** in 89% water) than obtained for the $Mn(III)_2(2\text{-}X(5\text{-}Y)salpn)_2$ (X = OH or H, Y = Cl or H) complexes (Table 1). The catalytic efficiencies of complex **6** (both in 89% water and 98% methanol) and the salpn complexes[39] are of similar order, all approximately 3 orders of magnitude lower than that of the catalase of *L. Plantarum* (Table 1).

The previously reported bimolecular rate constant for peroxide dismutation by complex **1** should be increased by 10-fold to take account of the 10-fold higher solubility of O_2 in methanol, the solvent employed for kinetic studies, versus that in water solvent. The solubilities were incorrectly assumed to be the same in that earlier work.

As discussed before[5,13,14,39] and above for complexes **1** and **7A**/**7A′**, a lower $Mn_2(II,II)/Mn_2(III,III)$ reduction potential is predicted to lead to a faster H_2O_2 disproportionation rate if oxidation of manganese is rate-limiting. No large difference in catalytic rate is observed between the $Mn(III)_2(2\text{-}X(5\text{-}Y)salpn)_2$ complexes versus the complexes **7A**/**7A′** and **6A**. The catalytic efficiency (k_{cat}/K_m) is comparable for these complexes and complex **6A** (Table 1). There is, however, a very large difference in the $Mn_2(II,II)/Mn_2(III,III)$ reduction potentials estimated[38,39] for the $Mn(III)_2(2\text{-}X(5\text{-}Y)salpn)_2$ complexes (between −618 and −270 mV) and the reduction potentials of complex **1** (+790 mV),[12] complex **7A** (+500 mV),[42] and complex **6** (+600 mV).[42] Yet the rate constant k_{cat} differs only modestly, between 4.2 and 21.9 for the salpn complexes versus 0.1, 0.65, and 2.7 for complexes **1**, **7A**/**7A′** and **6A**, respectively (Table 1). We conclude that reduction potential alone is not the determining factor in catalase rate acceleration of these model complexes. The principal factors in catalysis appear to be (1) the availability of an intramolecular base sufficiently basic to deprotonate H_2O_2 and (2) unobstructed substrate binding to the bridging site between the Mn ions as the deprotonated, end-on (μ,η_2) hydroperoxy anion. Substrate binding kinetics are thermodynamically coupled to deprotonation by intramolecular hydroxide ligands in both steps of substrate turnover. Substrate binding also requires μ-carboxylate conversion to terminal carboxylate as a means of maintaining a constant coordination number.[50]

Acknowledgment. We express our gratitude to Drs. S. V. Khangulov, G. Ananyev, Y. Abe, and K. Abe for insightful discussions. The research was supported by the U.S. National Institutes of General Medical Sciences (GM39932). A.E.M.B. acknowledges a fellowship from The Netherlands Organization for Scientific Research.

Supporting Information Available: Figure S1 showing the initial rate versus the hydrogen peroxide concentration for complex **1** and complex **1** + 1 equiv of hydroxide and Figure S2 showing the kinetics of hydrogen peroxide disproportionation for complex **1** + 5 equiv of hydroxide in water/methanol. This material is available free of charge via the Internet at http://pubs.acs.org.

IC9911771